Characteristics of Flame Propagation in Deflagration-to-detonation Process

Atsuhiro Kawamatsu, Kouki Tanabashi, Katsuo Asato,
Takeshi Miyasaka, Takuya Sukegawa, Yasuaki Kozato
Gifu University
1-1 Yanagido, Gifu, 501-1193, Japan

Key words: DDT, Vortex flow, Flame observation, Flame velocity

1 Introduction

A key problem in pulse detonation engines (PDEs) application is to achieve reliable and repeatable detonations in the shortest distance possible to minimize the system weight. A predetonator has been used to achieve shorter distance of deflagration-to-detonation transition (DDT) in the study [1]. However, the advantages of PDEs, such as their simplicity and low weight, are lost if devices such as a predetonator and an additional igniter are added. To control the DDT distance without the use of additional ignition energy and sophistication, heavy structures such as predetonators, efforts have been undertaken to apply the vortex flow (VF) injection concept to the injection part of a PDE, because the flame can propagate very quickly in a VF, depending on the rotating velocity [2, 3]. The DDT distance in a VF was shortened by 15-45 % compared with that in a counterflow [4]. Turbulence in a VF also promotes flame acceleration and shortens the DDT distance [5, 6]. In this study, the behavior of flame propagation was observed and the flame velocity and propagation velocity of the pressure wave in a detonation tube were measured to examine why the DDT distance in a VF was shortened and the location relative to the ignition spot for DDT.

2 Exprtimental Apparatus

Figure 1 shows a schematic of the experimental setup, which included the mixture supply, ignition system, measurement system and dump tank. An observation windows was installed at the location between x = 313 mm and x = 883 mm from the igniter. The mixture supplied into the detonation tube (diameter d = 76 mm) was ignited by the igniter installed at the closed end of the tube. The filling rate of the mixture was 90 % of detonation tube volume. The flame was propagated in the tube, and the burned gas was exhausted into the dump tank. The flame propagation process was observed using the Schlieren system with a high-speed video camera and ten pressure transducers and ion probes located at about 200-mm intervals. A hot-wire probe was inserted from a port in the pressure transducer, and the flow velocity in the tube was measured by a hot-wire anemometer.

Figure 2 shows the schematic structure of the VF injector. The fuel and oxidizer were supplied from the circumferential direction of the mixer tube where they were mixed. The mixture in the mixer tube was injected into the detonation tube from the circumference direction of the detonation tube. A

Correspondence to: asato@gifu-u.ac.jp

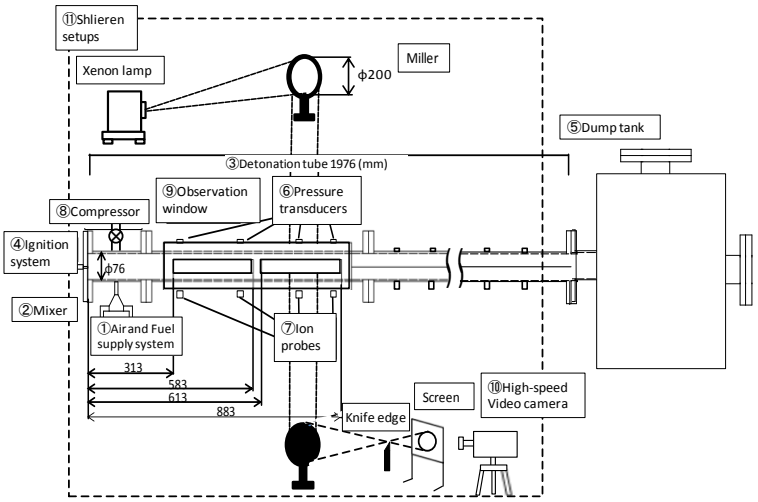

Figure 1. Experimental apparatus

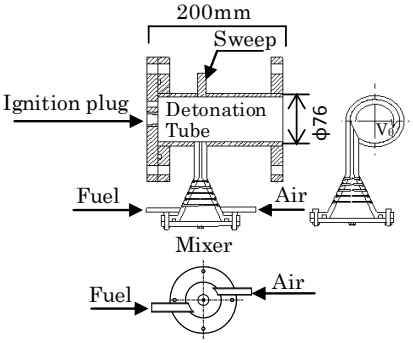

Figure 2. Structure of Vortex-flow (VF) type injector

VF field was then established in the detonation tube. The Shchelkin spiral was inserted between x = 0 mm and x = 520 mm in this experiment. The length (L_{ss}) and blockage ratio (BR) of the Shchelkin spiral were L_{ss} = 520 mm and BR = 40.4 %, respectively. Experiments both with and without the Shchelkin spiral were carried out. The effects of only VF and the combined effects of a VF and the Shchelkin spiral on the DDT process were examined. Hydrogen and air (equivalence ratio φ = 1.0) were used as the fuel and oxidizer, respectively.

3 Experimental Results and Discussion

Figure 3 shows the Schlieren photographs of flame propagation with the Shchelkin spiral. The field of vision is between x = 313 mm and x = 583 mm at the upstream part of the observation windows. Some white line patterns, which are indicated by the arrows and appear to be the pressure wave, can be seen in the space of the Shchelkin spiral, as shown in Fig. 3-(4) ~ (10). The flame, which is shown as the black image, appears behind the white line patterns in Fig. 3-(5) ~ (19). The flame joins the white line patterns at the end of the Shchelkin spiral in Fig. 3-(12) and (13), and then the flame and white line patterns propagate together, as shown in Fig. 3-(13) ~ (16).

Figure 4 shows the variation of the pressure and ionization current signals with the elapsed time at port 1 (x = 340 mm) and port 2 (x = 540 mm). The numbers and yellow and black lines in Fig. 4 correspond to those in Fig. 3. The abscissa gives the elapsed time from when the pressure wave has reached port 1. The pressure variation at port 2 is not observed until t = 0.192 ms. A large pressure variation is generated at t > 0.192 ms, which corresponds to Fig. 3-(13). After the flame joins the pressure wave and reaches port 2, as shown in Figs. 3-(13) and (14), a large pressure increase appears repeatedly. The ionization current signal changes suddenly at t = 0.24 ms, which corresponds to Fig. 3-(15). When the pressure signal rises at t = 0.192 ms, the ionization current dose not change yet, indicating the flame propagates far behind the pressure wave.

Figure 5 shows the locations of the flame against the time. The flame velocity can be obtained from this result. The flame propagates at constant velocity in this region.

Figure 6 shows the flame velocities V_f, V_{fp}, V_{fp}' and the propagation velocity of the pressure wave V_p, respectively. V_f was obtained from the ionization current signals at the two neighboring ports. V_{fp} was calculated by differentiating the fitting curve in Fig. 5. $V_{fp}' = \Delta l_f/\Delta t_{fs}$ was calculated from the differential of the local flame locations, Δl_f, and the time obtained from the frame rate of the high-speed-camera, Δt_{fs}. V_f, V_{fp} and V_{fp}' remain nearly constant and have almost the same value as one another, but they do not reach the flame velocity of the C-J detonation [7]. The propagation velocity, V_p also fails to reach the value of the C-J detonation, $V_{pC\text{-}J}$ [7]. Therefore, the flame has not changed to the detonation in this region.

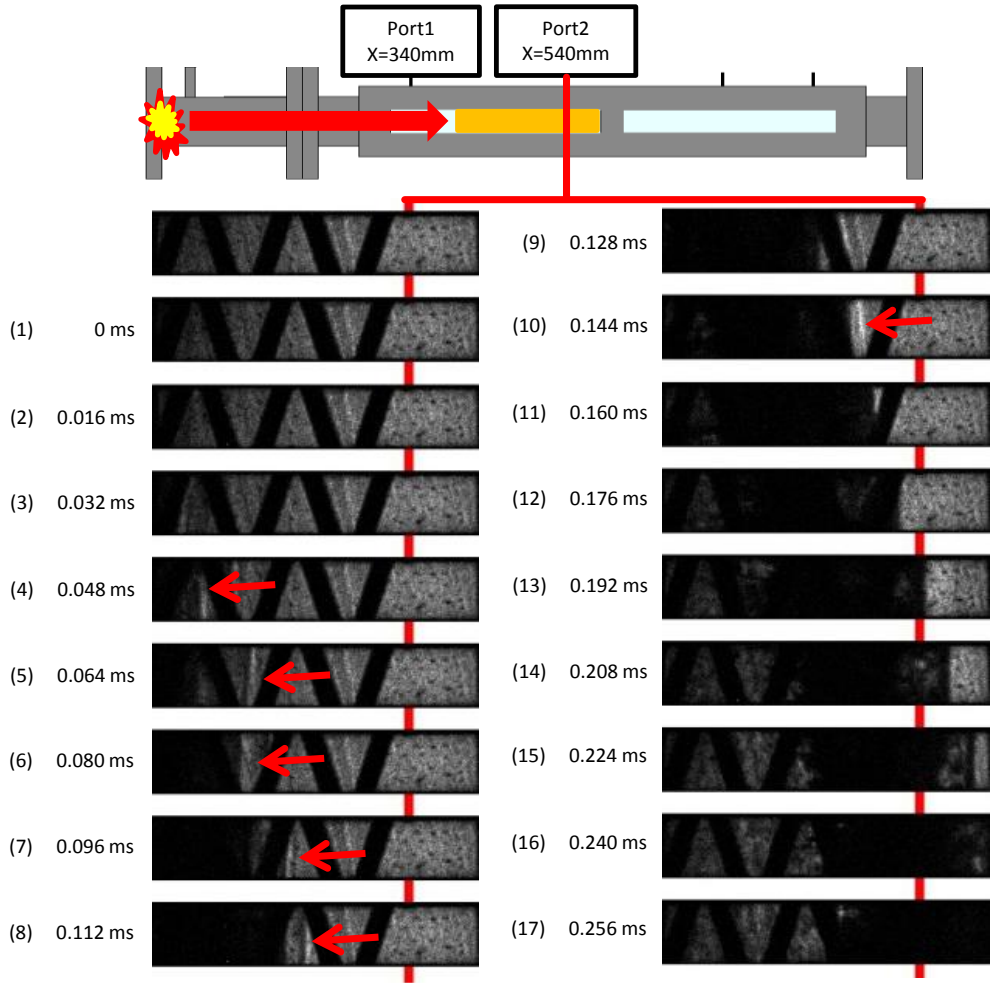

Figure 3. Flame propagation between port 1 and port2

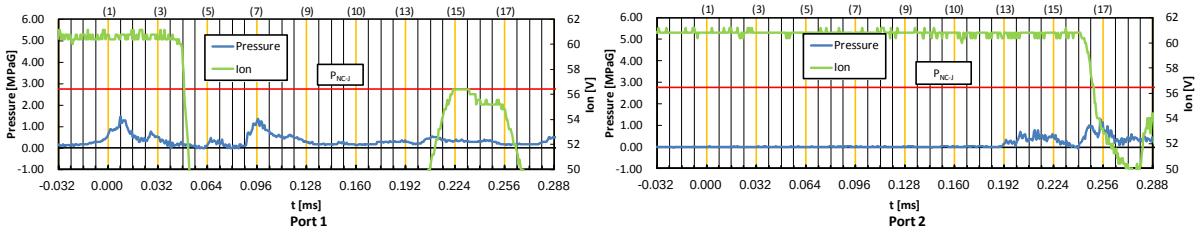

Figure 4. Pressure and ionization current signals at port 1 and pot 2

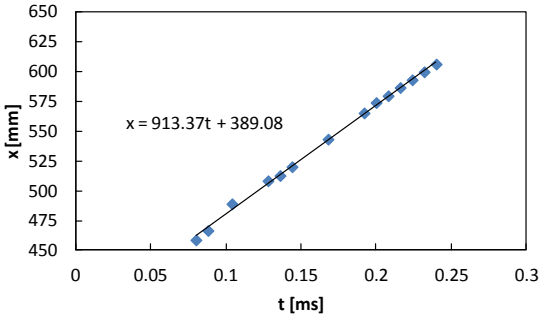

Figure 5. Locations of flame

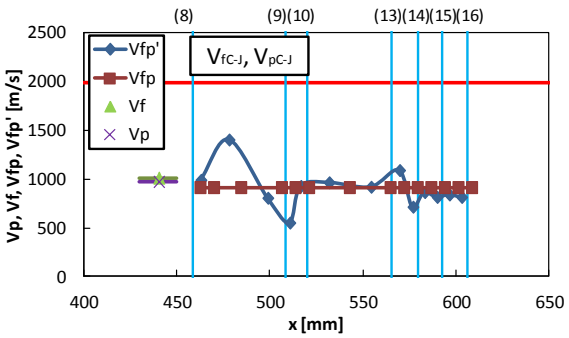

Figure 6. Flame velocity and propagation velocity of pressure wave between port 1 and port 2

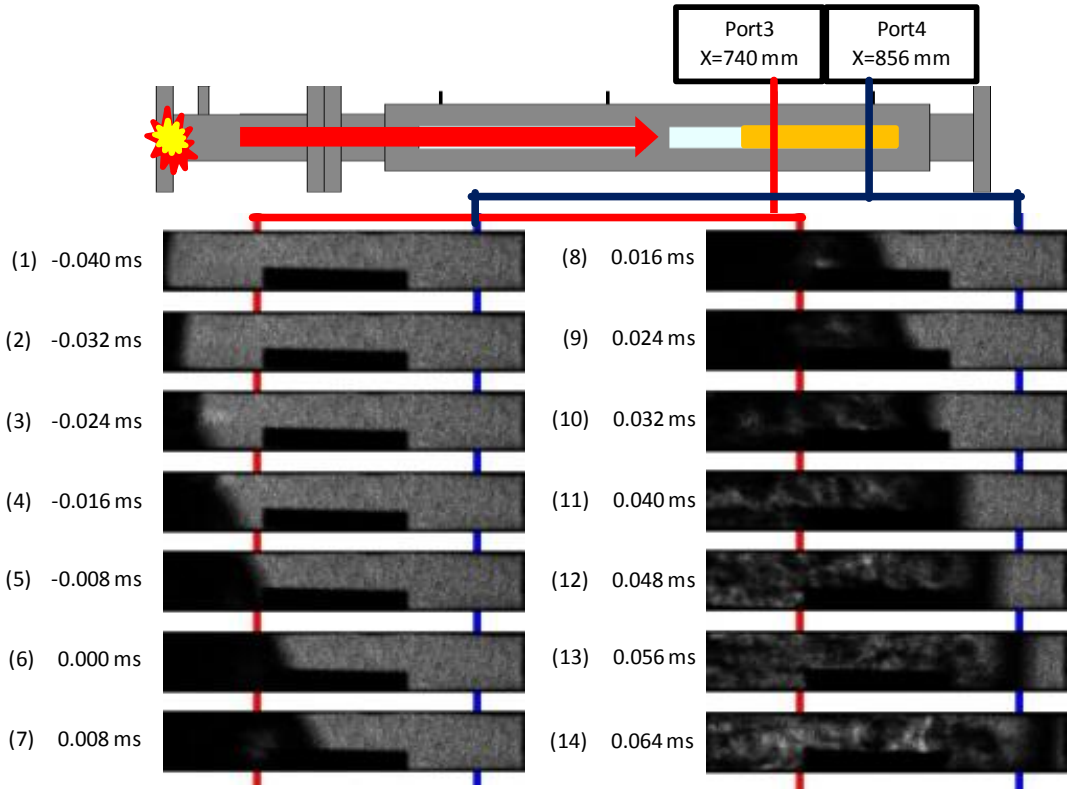

(a) Flame propagation between port 3 and port 4

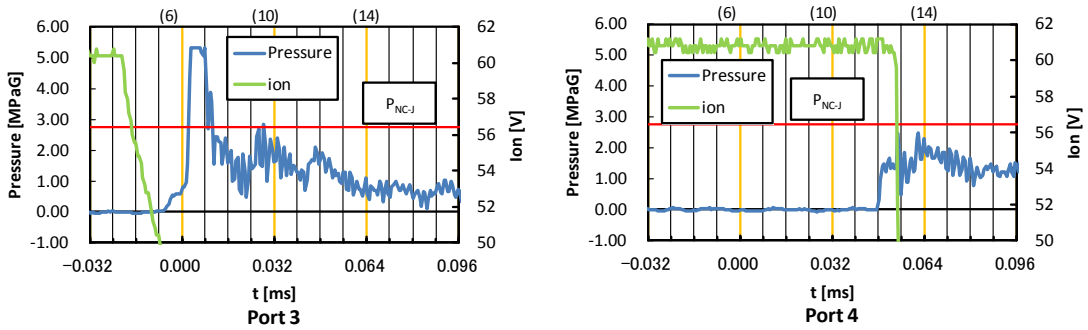

(b) Pressure and ionization current signals at port 3 and port4

Figure 7. Flame propagation, variation of pressure and ionization current signals at port 3 and port 4

Figure7 shows the flame propagation, pressure and ionization current signal. The visual field of the flame propagation is between x = 613 mm and x = 883 mm at the downstream part of the observation windows. The flame first propagates with the flat pattern and then diagonally and then flatly again. The pressure signal at port 3 rise at t = -0.008 ms, which corresponds to Fig. 7-(a)-(5). The flame also reaches port 3, because the ionization current signal has changed at this time. The ionization current signal starts to change at t = -0.022 ms which corresponds to Fig. 7-(a)-(3) ~ (4). The voltage of the ionization signal decreases from 60 V to 50 V at t = -0.008 ms, after that, the pressure at port 3 goes above the Neumann spike pressure of the C-J detonation [7]. This means that the deflagration has proceeded to the detonation near port 3 at t = 0 ms. The pressure and ionization current signals at port 4 suddenly change at t = 0.048 ms ~ 0.052 ms, which corresponds to Fig. 7-(a)-(12) or (13). The pressure at port 4 (x = 856 mm) has also reached the Neumann spike pressure of the C-J detonation, P_{NC-J}, when the detonation has reached port 4, as shown in Fig. 7-(a)-(12) or (13). The flame joins the pressure wave and then the flame and pressure wave propagate together.

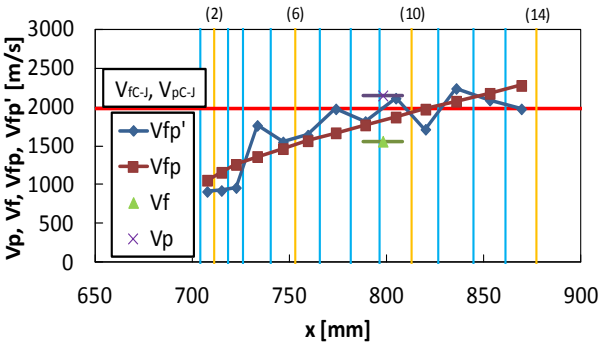

Figure 8. Flame velocity and propagation velocity of pressure wave between port 3 and port 4

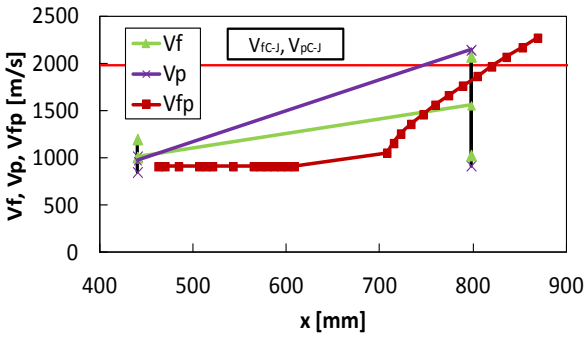

Figure 9. Flame velocity and propagation velocity of pressure wave in all areas of observation windows

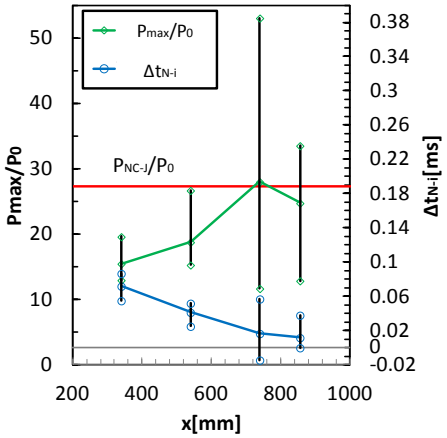

Figure 10. Variation of maximum pressures and differential in arrival times

Figure 8 shows the flame velocity with the Shchelkin spiral between x = 613 mm and x = 883 mm. V_f is about 1600 m/s, and V_{fp} is increased from about 1000 m/s to about 2250 m/s. This means that the flame has proceeded to the detonation in this region. $V_{fp}' = \Delta l_f/\Delta t_{fs}$ is rapidly increased with repeatedly increasing and decreasing. After that, the flame is rapidly accelerated between x = 740 mm and x = 800 mm, and then the deflagration has changed to the detonation in this region. V_p is about 2200 m/s, which goes above $V_{pC\text{-}J}$.

Figure 9 shows variation of V_f, V_{fp}, and V_p against the distance of x in all areas of the observation windows. V_f is about 1100 m/s at x = 440 mm and increases gradually until it reaches about 1600 m/s at x = 798 mm. On the other hand, V_{fp} is about 900 m/s and remains nearly constant between x = 440 mm and x = 600 mm. After that, V_{fp} is increased rapidly until about 2300 m/s at x = 832 mm. V_p increase until about 2200 m/s. V_{fp} and V_f reach the value of the C-J detonation at x = 856 mm.

Figure 10 shows the maximum pressure ratio, P_{max}/P_0, where P_0 is the atmospheric pressure. The maximum pressure ratio is initially about 15 ~ 20 and reaches about 30 at x = 856 mm, which is greater than the Neumann spike pressure $P_{NC\text{-}J}/P_0$ = 27 of the C-J detonation [7]. The differential in the arrival times between the flame and pressure wave, $\Delta t_{N\text{-}i}$ is initially about 0.07 ms. The flame propagates far behind the pressure wave between x = 340 mm ~ x = 600 mm. After that, $\Delta t_{N\text{-}I}$ become about 0.02 ms ~ 0.01 ms, and then the flame joins the pressure wave and they propagate together. The flame seems to proceed from deflagration to detonation at x = 755 mm ~ x = 830 mm, based on all the results of P_{max}/P_0, V_f, $V_{fp,}$ V_p and $\Delta t_{N\text{-}i}$.

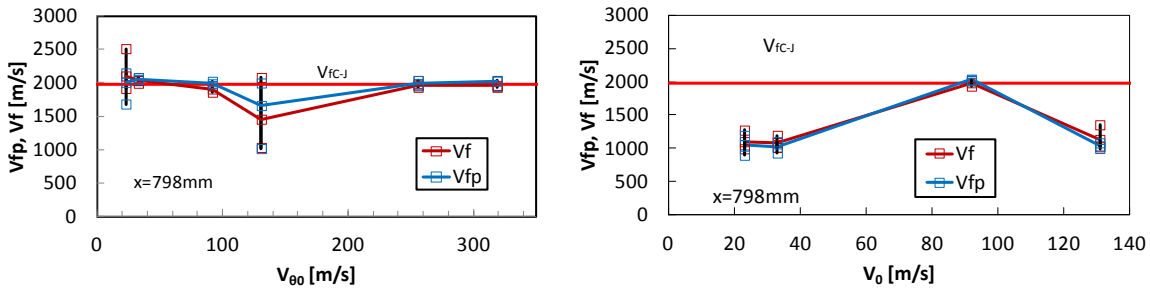

(a) Vortex flow (b) Counterflow

Figure 11. Flame velocity in vortex flow and counterflow when injection velocity was changed

Figure 11 shows the flame velocity V_{fp} and V_f when the injection velocity was changed. V_{fp} and V_f in a VF reach the value of the C-J detonation at x = 798 mm in all the cases of the injection velocity $V_{\theta 0}$, and the flame has changed from deflagration to detonation in this location. On the other hand, V_{fp} and V_f in a counterflow do not reach the value of the C-J detonation. The flame does not proceed to detonation in this location except V_0 = 92 m/s. The flame in a VF can change early from deflagration to detonation compared with that in a counterflow. It may be due to a strong turbulence generated in the tube by a VF. A turbulence and flow field in the tube should be measured to substantiate the above remarks.

4 Conclusions

The DDT process was examined by taking Schlieren photographs of flame propagation and measuring the pressure and ionization current. The following results were obtained;

(1) The flame velocity is rapidly increased when the Shchelkin spiral is inserted in the tube, and the flame proceeds from deflagration to detonation as it passes through the Shchelkin spiral. The combined effects of the VF and the Shchelkin spiral are effective and important for DDT.

(2) The flame in a VF changes early from deflagration to detonation compared with that in a countereflow. It may be due to a strong turbulence generated in the tube by a VF. The ignition spot, however, could not be found in this experiment.

References

[1] Frolov SM et al. (2005). Combined Strategies of Detonation Initiation in a Liquid-Fueled Air Breathing PDE. Proc. of Int. Symp. on Air Breathing Engine. CD-ROM. 2005-1292: 1.

[2] McCormack PD et al. (1972). Flame Propagation in aVortex Core. Combust. Flame. 19: 297.

[3] Asato K et al. (1997). Characteristics of Flame Propagation in a Vortex Core : Validity of a Model for Flame Propagation. Combust. Flame. 110 : 418.

[4] Asato,. K. Et al. (2012). Effects of a Vortex Flow on Characteristics of Deflagration-to-Detonation Transition, Trans. JSASS Aerospace. Tech. Japan, 10 (28) : 15.

[5] Kuo KK. (1986). Principles of Combustion. Jphn Wiley & Sons. New York (ISBN-471-09852-3).

[6] Oppenheim AK et al. (1963). Recent Progress in Detonation Research. AIAAJ. 1: 2243.

[7] Tanaka K. http://riodb.ibase.aits.go.jp/ChemTherm/aistjan.html